

RSC Advances



This is an *Accepted Manuscript*, which has been through the Royal Society of Chemistry peer review process and has been accepted for publication.

Accepted Manuscripts are published online shortly after acceptance, before technical editing, formatting and proof reading. Using this free service, authors can make their results available to the community, in citable form, before we publish the edited article. This *Accepted Manuscript* will be replaced by the edited, formatted and paginated article as soon as this is available.

You can find more information about *Accepted Manuscripts* in the [Information for Authors](#).

Please note that technical editing may introduce minor changes to the text and/or graphics, which may alter content. The journal's standard [Terms & Conditions](#) and the [Ethical guidelines](#) still apply. In no event shall the Royal Society of Chemistry be held responsible for any errors or omissions in this *Accepted Manuscript* or any consequences arising from the use of any information it contains.

1 **Paraffin confined in carbon nanotubes as nano-encapsulated phase change**
2 **materials: Experimental and molecular dynamics studies**

3

4 Changda Nie, Xuan Tong, Shuying Wu*, Shuguang Gong, Deqi Peng

5 School of Mechanical Engineering, Xiangtan University, Xiangtan 411105, Hunan

6 Province, PR China

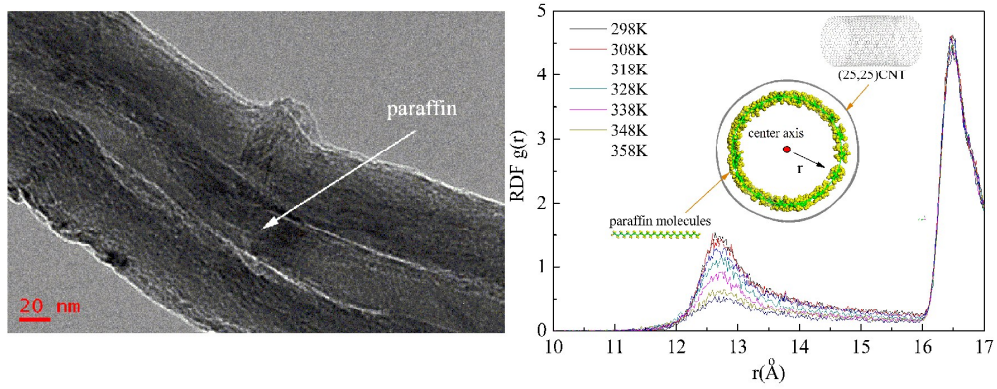
7 *Corresponding authors:

8 Shuying Wu, E-mail: wusy2015@126.com; Tel.: +86 731 58292209

9

10 **Graphic abstract**

11



12

13

14

15

16 **Abstract**

17 The characteristic of paraffin confined in carbon nanotubes (CNTs) was
18 investigated with experimental and molecular dynamics (MD) methods. Through a
19 vacuum infiltration process, paraffin was successfully infiltrated into the inner space
20 of CNTs, which was proved by TEM and DSC observations. The melting point and
21 latent heat were both lower than the bulk. Furthermore, MD simulations were
22 performed to provide insight about the structure distribution of paraffin confined in
23 CNTs and to attempt an explanation of the experimental results. The MD simulation
24 results indicated that paraffin molecules exhibited an orderly structure distribution
25 near the inner wall of CNTs, which gradually turned disorderly with increasing
26 temperature. The self-diffusion coefficient compared with pure paraffin increased.
27 These behaviors could be attributed to the nano-confined environment of CNTs and
28 the interaction between paraffin molecules and the tube walls. The current research is
29 significant for understanding the behaviors of alkane-based phase change materials
30 inside CNTs, which could provide new applications of paraffin in microelectronics
31 cooling.

32

33 **Keywords:** paraffin; carbon nanotubes; confined; phase change material; molecular
34 dynamics.

35

36

37 **1 Introduction**

38 The continuing miniaturization and light weight of electronic and mechanical
39 devices is accompanied with a dramatic rise of heat flux per unit volume. Therefore,
40 how to cool effectively and quickly becomes the key issues. The liquid coolant is
41 often mentioned for cooling microelectronics in recent reports.^{1,2} The addition of high
42 thermal conductive particles to liquid coolants holds great promise for enhancing the
43 cooling effect.³

44 Carbon nanotubes (CNTs) have received considerable attention for a long time,
45 due to their remarkable physical properties, such as a high thermal conductivity of
46 2000~6000 W/m·K.⁴ Meanwhile, the hollow cylindrical structure is another important
47 feature of CNTs. Various liquid materials could be infiltrated into the hollow structure
48 if the surface tension of the liquid is below 200 mN·m⁻¹,⁵ for example, water,
49 polymers and also paraffin. Many materials have been shown unconventional
50 behaviors when confined in CNTs, such as experiencing a liquid-solid transition at
51 room temperature for water.⁶ Paraffin, with high latent heat, low cost, stability,
52 nontoxicity and resistivity to corrosion, has been widely used as phase change
53 materials (PCMs) in industrial fields.⁷ A latest usage for paraffin is intercalated into
54 CNTs and then dispersed into liquid coolant to enhance the heat transfer rate and
55 decrease temperature of microelectronic.⁸ Due to the PCM fusion, an additional
56 reduction in temperature of CNTs filled with nano-encapsulated wax could be realized
57 comparing with CNT suspensions. Meanwhile, the intercalation of different types of
58 paraffins and their mixtures with triglycerides inside CNTs could realize a smart

59 tunable working temperature.⁹ In the intercalation experiment, paraffin outside CNTs
60 could be completely removed with proper solvent treatment, while that inside CNTs
61 won't be washed away.¹⁰ Unfortunately, to date, the related experimental data is very
62 limited. Meanwhile, the mechanism by which these paraffin molecules confined in
63 CNTs is poorly understood.

64 Recently, with the rapid development of molecular dynamics (MD), it has been
65 widely used to predict the thermophysical properties of various materials¹¹ and
66 explain some phenomena, such as the driving force for the filling of CNTs with
67 water,⁶ the melting behavior of alkane as phase change materials slurry¹² and the
68 interaction between surfactant molecules and CNTs.¹³ Sosso et al.¹⁴ simulated the fast
69 crystallization process of phase change compound GeTe. Rao et al.¹⁵ tried to interpret
70 the mesostructures and morphology evolution of the nano-encapsulated PCM by
71 simulation method. Therefore, MD simulation seems to be a very suitable tool in
72 studying the characteristic of PCMs confined in CNTs.

73 In this paper, the encapsulation of paraffin inside CNTs was successfully realized
74 by the vacuum infiltration method. The phase change properties were investigated by
75 DSC measurements. Also, we attempted to investigate the interaction between CNTs
76 and PCMs, the structure distribution and self-diffusion coefficient of paraffin confined
77 in CNTs with MD methods.

78 **2 Methods**

79 **2.1 Experimental methods**

80 **2.1.1 Opening the ends of CNTs**

81 The pristine CNTs (Chengdu Organic Chemicals Co., Ltd., China) were
82 suspended in refluxing nitric acid solution at 120 °C for 4 h, then filtered and washed
83 thoroughly with distilled water until the filtrate was neutral. Finally, the opened-end
84 CNTs were dried in a vacuum oven at 60 °C for 24 h.

85 **2.1.2 Infiltrating CNTs with paraffin**

86 The paraffin wax (melting point: 53-55 °C) used in the experiment was supplied
87 by Shanghai Huashen Recover Equipment Co., China. A solution of paraffin in
88 benzene with a weight ratio of 1:4 was prepared. The solution was sonicated for 10
89 min until the solute was fully dissolved. Meanwhile, the opened-end CNTs were put
90 into a flask. The air in the flask was removed by a vacuum pump. Also, the air
91 contained inside CNTs was removed, which facilitated the liquid paraffin to rapidly
92 infiltrate CNTs. Then, the solution was injected into the flask and maintained for 20
93 min at 80 °C. In this process, it was predicted that there was only little paraffin filling
94 in CNTs due to the equal pressure of inside and outside of CNTs. Thus, the pressure
95 of the flask was rapidly increased to 1 atm, which could make massive paraffin
96 infiltrate CNTs.¹⁰ This process maintained for 30 min. Plenty of benzene would be
97 evaporated in this process due to the solution temperature above its boiling point,
98 which meant the self-sustained diffusion took place.⁹ The mixture in the flask were
99 filtered and cleaned by hot benzene with 2~3 times to remove the residual solute
100 deposited on the outside of CNTs. Finally, the sample was dried in a vacuum oven at
101 40 °C for 2 h.

102 **2.1.3 Characterization**

103 Transmission electron microscopy (TEM) (JEM-2100F) analyses were
104 performed to determine the microstructures of CNTs and paraffin confined in CNTs.¹⁶
105 A suspension was prepared by dispersing CNTs or CNTs filled with paraffin into
106 ethanol and ultrasonicated for 10 s. Then, the test samples were obtained by adding a
107 drop of the suspension to a holey copper grid that had holes 1.2 μm in size.

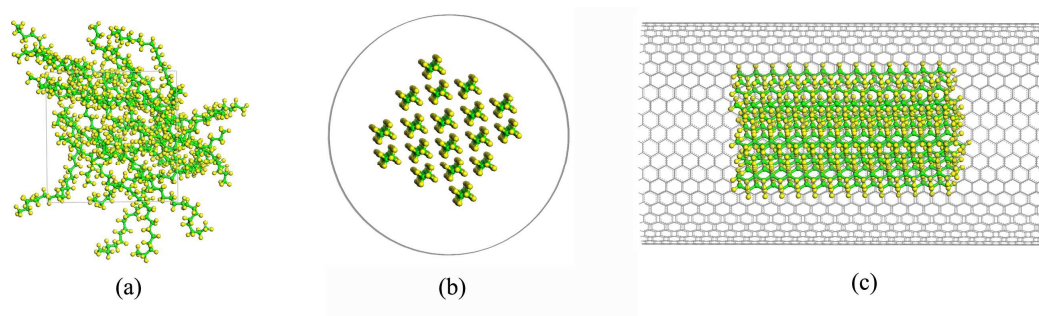
108 The thermal performance of paraffin and paraffin confined in CNTs were
109 measured using a differential scanning calorimeter (DSC-Q10, TA Instrument Inc.,
110 USA) under N_2 atmosphere with a scanning rate of 5 $^\circ\text{C}/\text{min}$ in the temperature range
111 of 25 $^\circ\text{C}$ to 75 $^\circ\text{C}$.

112 Infrared spectra of the samples were recorded using an attenuated total reflection
113 (ATR) method with a Fourier transform infrared spectrometer (FTIR) (Nicolet 6700)
114 in the range of 4000~600 cm^{-1} .

115 **2.2 MD Simulations**

116 MD simulations were performed using Amorphous Cell, Discover and Forcite
117 modules incorporated in Materials Studio software with the condensed-phase
118 optimized molecular potential for atomistic simulation studies force field. For paraffin
119 system, *n*-hexacosane was chosen to represent paraffin according to the DSC
120 measurement results. For CNTs system, although multi-wall CNTs were used in the
121 experiment, the model of single-wall CNT was built in the simulation because here
122 we mainly concerned on the interaction of paraffin and inner wall of CNT.¹³
123 Meanwhile, it could reduce the computation load by using single-wall CNT. Finally,
124 models of an opened-end (25, 25) CNT, total of 2500 carbon atoms in box with a size

125 of $37.2 \times 37.2 \times 61.5 \text{ \AA}$, and paraffin system, composed of 18 *n*-hexacosane
126 molecules with a size of $23.9 \times 23.9 \times 23.9 \text{ \AA}$, were built. To obtain the initial
127 structure of paraffin confined in CNTs, 18 *n*-hexacosane molecules, calculated
128 according to the degree of filling of paraffin in the experiment, were embedded in (25,
129 25) CNT. The initial configurations of the simulated systems are shown in Fig. 1.



130

131 **Fig. 1.** The illustration of the computational model: *n*-hexacosane (a), (25, 25) CNT
132 filled with *n*-hexacosane with the cross-sectional view (b) and the side view (c)

133 After the initial structures were constructed, the smart minimization method was
134 used to optimize the geometry. System equilibrations were performed over 200 ps for
135 paraffin and confined paraffin in constant-pressure, constant-temperature (NPT)
136 ensemble at $T = 298 \text{ K}$ and $p = 1 \text{ atm}$. After that, three anneal cycles were performed
137 in order to eliminate unstable conformations, heating systems from 298 K to 358 K in
138 a speed of 1 K/ps then cooling down in the same speed. When the system achieved an
139 equilibration state, the melting process was performed from 298 K to 358 K with a
140 temperature increment of 10 K. At each temperature, the system should be
141 pre-equilibrated with a 200 ps run before the data collection in the next 200 ps. The
142 time step was 1 fs and the periodic boundary conditions were applied in the above
143 simulation. Andersen's thermostat and Berendsen's barostat methods were used to

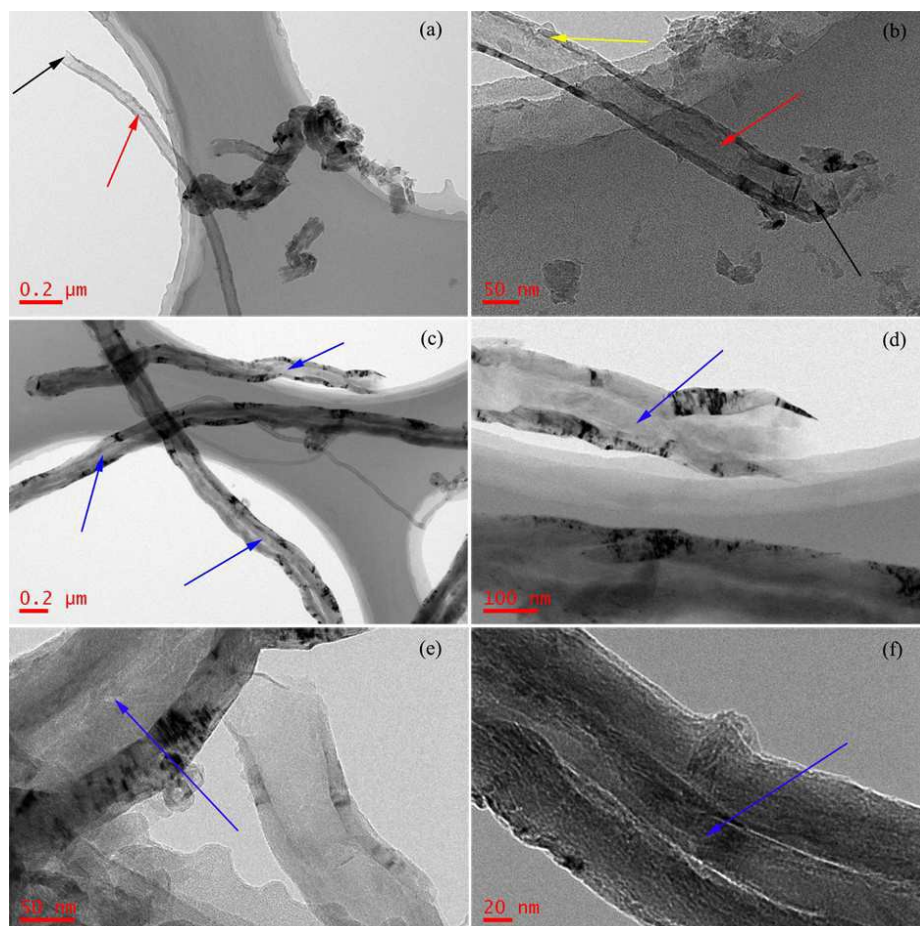
144 control temperature and pressure, respectively.

145 3. Results and discussions

146 3.1. Analysis of TEM

147 The TEM observations are performed to investigate if paraffin is filled in CNTs
148 or not.¹⁰ Fig. 2 (a) and (b) show TEM images of CNTs after the acid treatment. It
149 obviously shows that the tips of CNTs are removed and CNTs are effectively opened,
150 which allows the molten paraffin to infiltrate CNTs. In Fig. 2 (b), one could see that
151 the CNT wall is partially eroded by the nitric acid treatment.

152 Fig. 2 (c), (d), (e) and (f) show that paraffin is successfully infiltrated into CNTs.



153

154 **Fig. 2.** TEM images of opened-end CNTs (a-b) and CNTs filled with paraffin (c-f).

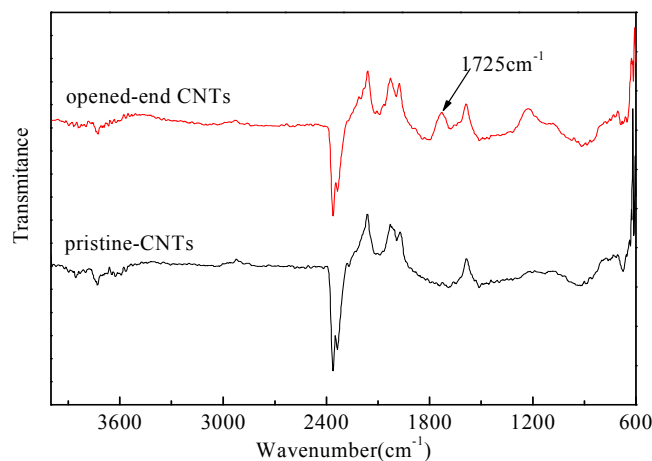
155 The black arrows indicate the opened ends. The red arrows indicate the empty cavity.
156 The yellow arrows indicate the erosion location. The blue arrows indicate paraffin
157 filled in CNTs.

158 There is almost no paraffin deposited on the outside of tubes due to being cleaned by
159 benzene. However, the outflow of paraffin filled in the inside is difficult during the
160 benzene-cleaned process. According to the open literatures,¹⁷⁻¹⁹ the nonoutflow is
161 likely to occur when the pore size is in the mesoporous range 2~50 nm, while the
162 outflow is relatively easy if the pore size is smaller than about 1~2 nm. The inner
163 diameter of CNTs used in this work is 20~50nm, which is in the range of nonoutflow.
164 The nonoutflow behavior is very complicated, affected by pressure, surface and
165 interfacial properties, and other factors.

166 3.2. Analysis of FT-IR

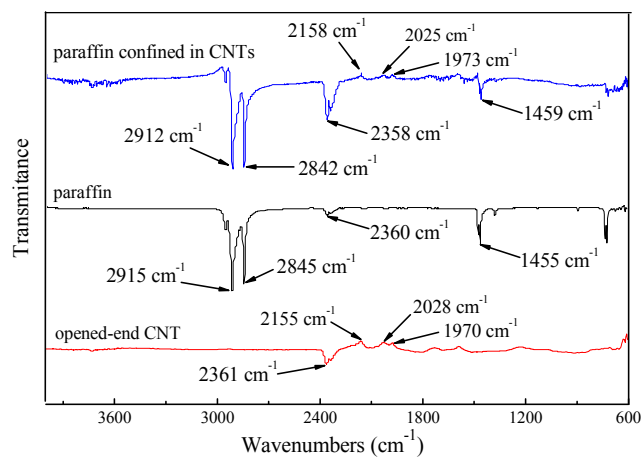
167 The FT-IR spectra of several samples are shown in Fig. 3 and 4. Compared with
168 the spectrum of pristine CNTs in Fig. 3, it gets a new peak at 1725 cm^{-1} due to the
169 C=O stretching indicating the presence of carboxyl groups after the acid treatment.²⁰
170 As presented in Fig. 4, four remarkable peaks are found in the spectra of paraffin. The
171 vibration spectra observed at 2845 and 2912 cm^{-1} are ascribed to the C-H stretching
172 vibration of CH_3 and CH_2 . The absorption bands obtained at 1459 and 717 cm^{-1} are
173 primarily assigned to C-H bending vibration and in-plane deformation rocking
174 vibration of paraffin molecular, respectively. No significant new peaks are formed in
175 paraffin confined in CNTs, whose spectrum is just the spectrum stack of paraffin and

176 opened-end CNTs. The FT-IR spectrum proves that it is a physical interaction
 177 between paraffin and CNTs and



178

179 **Fig. 3.** FT-IR spectra of pristine-CNTs and opened-end CNTs



180

181 **Fig. 4.** FT-IR spectra of paraffin, opened-end CNTs and paraffin confined in CNTs

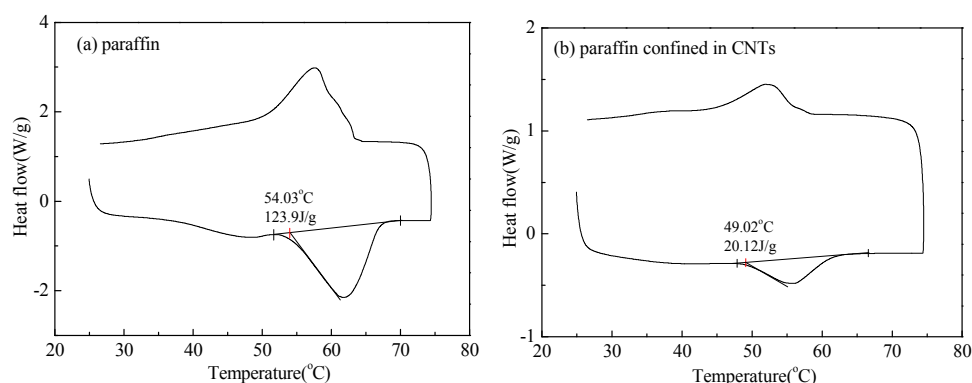
182 there is no chemical reaction in the infiltrating process.

183 3.3 Analysis of DSC

184 DSC thermograms of paraffin and paraffin confined in CNTs are presented in
 185 Fig. 5. The melting temperature was estimated by the tangent at the point of greatest
 186 slope on the face portion of the peak of the DSC curve. The latent heat of phase

187 change was determined by numerical integration of the area under the peaks. It is
188 observed that the melting point of paraffin decreases from 54.03 to 49.02 °C after it
189 infiltrated CNTs. The similar phenomenon was found in the literatures,^{9, 10} which is
190 due to the extreme confinement of the nanometer-size CNTs.²¹

191 The latent heats of fusion of 123.9 J/g and 20.12 J/g are obtained for paraffin and
192 paraffin confined in CNTs, respectively. According to the latent heat values, the



193

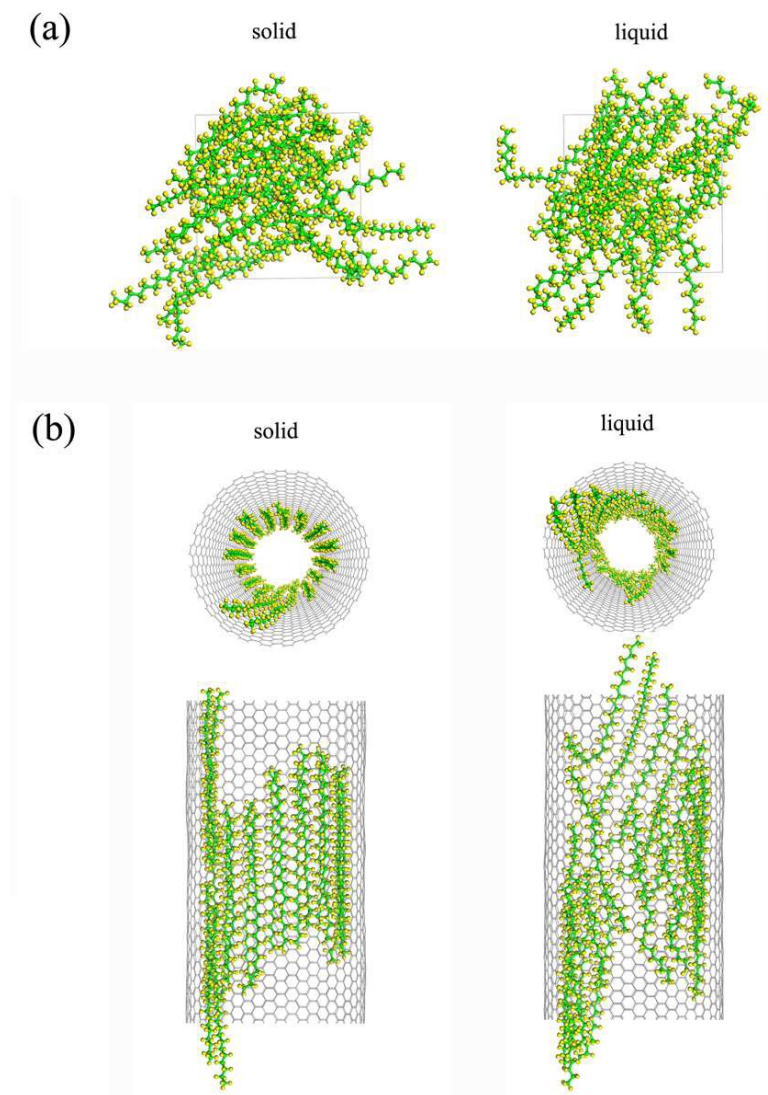
194 **Fig. 5.** DSC of (a) paraffin and (b) paraffin confined in CNTs

195 intercalated mass fraction of paraffin confined in CNTs was 16.24%. It is slightly
196 higher than that of pure paraffin and slightly lower than that of mixing paraffins
197 intercalated in CNTs reported by Sinha-Ray.⁹ Compared with the mass fraction, the
198 degree of filling,²² which is defined as the volume of paraffin vs the volume of empty
199 tubes of CNTs, could better reflect the availability of the empty tubes of CNTs. As the
200 mass of paraffin confined in CNTs is 3.1 mg, the total mass of paraffin in CNTs is
201 calculated to be 0.5034 mg. According to the TEM observations, the CNTs have an
202 ID 20~50 nm, an OD 30~60 nm and a length 1~10 μm . These data are used to
203 calculate the degree of filling of paraffin filled in CNTs. The paraffin density is 0.9
204 $\text{g}\cdot\text{cm}^{-3}$ and the CNT density is $1.6\text{ g}\cdot\text{cm}^{-3}$.⁸ Correspondingly, the volume of paraffin

205 filled in CNTs is $1.263 \times 10^{-15} \text{ cm}^3$. The total volume of the empty tubes of CNTs is
206 $4.808 \times 10^{-15} \text{ cm}^3$. Ultimately, the degree of filling of paraffin inside CNTs is 26.27%,
207 which indicates the complete filling is not obtained and the volume of paraffin filled
208 in CNTs could be further improved. This pattern is consistent with the results reported
209 by Bazilevsky et al.²³ who showed that the competition of Brownian diffusion and
210 intermolecular forces would affect the degree of filling.

211 **3.4 The structure of paraffin confined in CNT**

212 The structure of materials has an important effect on their properties. To reveal
213 the corresponding properties and the paraffin-CNT interaction, the structures of
214 paraffin in a freestanding state and inside CNT are analyzed in detail by MD method.
215 As shown in Fig. 6, there is a large structural difference between them both in the
216 liquid and solid states, of which the final structures are obtained after running 1000



217

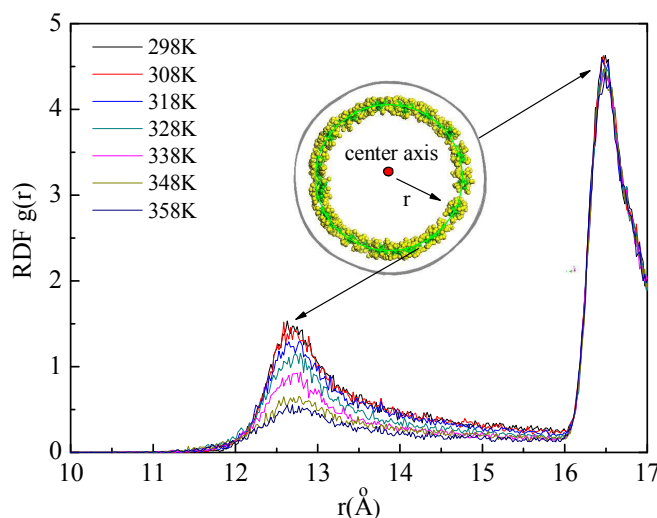
218 **Fig. 6.** The structures of paraffin in freestanding state (a) and confined in CNT (b)

219 ps dynamic simulations at 298 K and 358 K respectively. Obviously, the structures of
220 paraffin confined in CNT are more orderly than those with the freestanding state due
221 to the confinement of CNT. Meanwhile, in the freestanding state and inside CNT, the
222 paraffin molecules with the solid state are more orderly than those with liquid state
223 due to the thermal motion of molecules. When paraffin confined in CNT, the paraffin
224 molecules are almost spaced one by one and orientated along the CNT inner wall,

225 instead of occupying the center of CNT. The ordered molecule structures inside CNT
226 have been previously predicted by the simulations and experiments.²⁴⁻²⁶ Jiang et al.
227 stated that the Fe melts became orderly in nano-confined environment due to the
228 inductive effect of CNT.²⁵

229 3.5 Radial distribution

230 The radial distribution function (RDF, $g(r)$), representing the probability of a
231 particle at a distance of r away from another referenced particle, is often used to
232 provide insight into the interaction between two similar or different species.²⁷ Fig. 7
233 shows the RDF of carbon atoms of paraffin molecules and CNT around the axis of the
234 tube at different temperatures. With the increase of temperature, the height of the peak
235 decreases slightly and the width of the peak increases slightly. The variety of peak
236 intensity indicates the changes of the order parameter. The motion of paraffin
237 molecules in CNT increased and the degree of order decreased, which is consistent
238 with the solid-liquid phase transition of paraffin from an ordered to a disordered



239

240 **Fig. 7.** RDF of carbon atoms around the axis of the tube for paraffin confined in CNT

241 process.

242 The average values of two peaks at different temperatures are observed about
243 12.7 and 16.5 Å, respectively. The first peak means the position of carbon atoms of
244 paraffin molecules and the second peak is related to the position of carbon atoms of
245 CNT. The distance between the paraffin molecules and tube wall of CNT keeps at 3.8
246 Å, which result in the interaction of paraffin molecules-CNT wall. We considered that
247 the mainly interaction force should be the van der Waals force,²⁸ which makes
248 paraffin molecules orderly distribute along the inner wall of CNT and nonoutflows
249 from the inner space.

250 3.6. Self-diffusion coefficient

251 In order to understand the diffusion behavior of paraffin molecules in the
252 nano-confined environment, the self-diffusion coefficient D is calculated in the
253 simulation, which can be obtained by the Einstein equation:

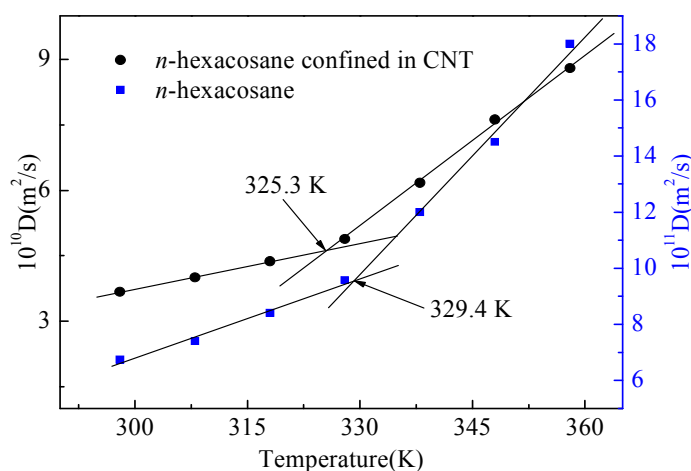
$$254 \quad D = \frac{1}{6N} \lim_{t \rightarrow \infty} \frac{d}{dt} \sum_{i=1}^N \left\langle \left| r_i(t) - r_i(0) \right|^2 \right\rangle \quad (1)$$

255 where N is the number of atoms, t is the simulation time, r_i denotes the position
256 vector of i th particle, and the angular brackets denote the ensemble average. The value
257 of self diffusion coefficient is evaluated by the limiting slope of the mean square
258 displacement, which is obtained as a function of time.¹²

259 The self-diffusion coefficient as a function of temperature is shown in Fig. 8. It
260 shows that the self diffusion coefficient of both systems increases with the increase of
261 temperature, due to the kinetic energy increasing with temperature. As presented by
262 Rao et al.,¹² the turning point of the self-diffusion coefficient is regarded as the phase

263 change temperature of *n*-alkane. So, the phase change temperatures of paraffin system
 264 and paraffin confined in CNT system are 329.4 and 325.3 K, respectively. The
 265 experimental values measured by DSC method in 3.3. section are 327.18 and 322.17
 266 K. The differences between the MD simulation and experimental results are 0.67%
 267 and 0.96%, respectively. Hence, it indicates that MD simulation is proper to
 268 investigate the properties of the current systems.

269 Meanwhile, it is found that the self-diffusion coefficient of the confined
 270 paraffin is higher than that of bulk paraffin. It means the mobility strength of the
 271 molecules increases in the nano-confined environment, which would lead to the
 272 increase of heat transfer rate.²⁹ Zheng et al. also stated that the self-diffusion
 273 coefficient of the confined water exhibited an unexpected increase inside the large
 274 CNT compared to that of bulk water.³⁰ This phenomenon may be due to the mutual
 275 defects of the small confinement and the nanoscale surface of CNT.



276

277 **Fig. 8.** The self-diffusion coefficient as a function of temperature

278 **4 Conclusions**

279 A combined method based on experiments and MD simulations was carried out
280 to study the behavior of paraffin infiltrated in CNTs. An encapsulated phase change
281 material of paraffin filled in CNTs was prepared by the vacuum infiltration method.
282 TEM and DSC observations proved that paraffin was successfully infiltrated into the
283 inner space of CNTs. Moreover, MD simulations were used to probe properties of
284 paraffin filled into CNT. Compared with bulk paraffin, a lower melting point was
285 found by MD simulation, which was in agreement with the experimental results.
286 Different from the disordered structure of bulk paraffin, paraffin molecules were
287 orientated orderly along the CNT inner surface. With the increase of temperature, the
288 degree of order decreased. The main interaction between CNTs and paraffin
289 molecules should be the van der Waals force. The self-diffusion coefficient of the
290 confined paraffin exhibited an increase inside the CNTs compared to that of bulk
291 paraffin. The results suggest that the nano-confined environment of CNT and the
292 interaction between paraffin molecules and the confining wall play an important role
293 in the structure and thermal properties of paraffin confined in CNTs.

294 **Acknowledgements**

295 The work was supported by the National Nature Science Foundation of China
296 (Grant 51206071), the China Postdoctoral Science Foundation (Grant 2013M542125)
297 and the Hunan Provincial Natural Science Foundation of China (Grant 13JJ6040).

298 **References**

- 299 1 C.S. Best., 2014, *US0307384 A1*.
- 300 2 C.S. Sharma, G. Schlottig, T. Brunschwiler, M.K. Tiwari, B. Michel and D. Poulikakos, *Int. J.*
301 *Heat Mass Tran.*, 2015, 88, 684-694.
- 302 3 S.S.J. Aravind and S. Ramaprabhu, *RSC Adv.*, 2013, 3, 4199-4206.

- 303 4 J.E. Fischer, *CRC press*, 2006.
- 304 5 D.A. Britz and A.N. Khlobystov, *Chem. Soc. Rev.*, 2006, 35, 637-659.
- 305 6 T.A. Pascal, W.A. Goddard and Y. Jung, *P. Natl. Acad. Sci.*, 2011, 108, 11794-11798.
- 306 7 Q.Q. Tang, J. Sun, S.M. Yu, G.C. Wang, *RSC Adv.*, 2014, 4, 36584-36590.
- 307 8 S. Sinha-Ray, S. Sinha-Ray, H. Sriram and A.L. Yarin, *Lab Chip*, 2014, 14, 494-508.
- 308 9 S. Sinha-Ray, R.P. Sahu and A.L. Yarin, *Soft Matter*, 2011, 7, 8823-8827.
- 309 10 N. Jeong, Y.C. Park and J.H. Yoo, *Carbon*, 2013, 63, 240-252.
- 310 11 K. Lindorff-Larsen, *Biophys. J.*, 2015, 108, 380a.
- 311 12 Z. Rao, S. Wang, M. Wu, Y. Zhang and F. Li, *Energy Convers. Manage.*, 2012, 64, 152-156.
- 312 13 B. Sohrabi, N. Poorgholami-Bejarpasi and N. Nayeri, *J. Phys. Chem. B*, 2014, 118, 3094-3103.
- 313 14 G.C. Sosso, G. Miceli, S. Caravati, F. Giberti, J. Behler and M. Bernasconi, *J. Phys. Chem. Lett.*,
314 2013, 4, 4241-4246.
- 315 15 Z.H. Rao, X.Y. You, Y.T. Huo, X.J. Liu, *RSC Adv.*, 2014, 4, 39552-39557.
- 316 16 Z.Y. Hu, J.J. Zhao, Z.Z. Song, C.P. Yang, *RSC Adv.*, 2015, 5, 16792-16800.
- 317 17 A. Han, X. Kong and Y. Qiao, *J. Appl. Phys.*, 2006, 100, 014308.
- 318 18 A. Han and Y. Qiao, *Langmuir*, 2007, 23, 11396-11398.
- 319 19 W. Lu, V.K. Punyamurtula and Y. Qiao, *Int. J. Mater. Res.*, 2011, 102, 587-590.
- 320 20 J. Wang, Z. Dong, J. Huang, J. Li, X. Jin, J. Niu, J. Sun and J. Jin, *Appl. Surf. Sci.*, 2013, 270,
321 128-132.
- 322 21 A.V. Bazilevsky, K. Sun, A.L. Yarin and C.M. Megaridis, *J. Mater. Chem.*, 2007, 18, 696-702.
- 323 22 V.D. Borman, A.A. Belogorlov, A.M. Grekhov and V.N. Tronin, *Eur. Phys. J. E. B*, 2014, 87,
324 1-18.
- 325 23 A.V. Bazilevsky, K. Sun, A.L. Yarin and C.M. Megaridis, *Langmuir*, 2007, 23, 7451-7455.
- 326 24 G. Hummer, J.C. Rasaiah and J.P. Noworyta, *Nature*, 2001, 414, 188-190.
- 327 25 Y.Y. Jiang, H. Li, K. Zhang, H.Q. Yu, Y.Z. He and X.G. Song, *EPL-Europhys. Lett.*, 2012, 97,
328 16002.
- 329 26 X. Liu, X. Pan, S. Zhang, X. Han and X. Bao, *Langmuir*, 2014, 30, 8036-8045.
- 330 27 G. Zhou, T. Zhao, J. Wan, C. Liu, W. Liu and R. Wang, *Carbohydr. Res.*, 2015, 401, 89-95.
- 331 28 Y. Jiang, K. Zhang, H. Li, Y. He and X. Song, *Nanoscale*, 2012, 4, 7063-7069.
- 332 29 K.S. Hwang, S.P. Jang and S.U.S. Choi, *Int. J. Heat Mass Tran.*, 2009, 52, 193-199.
- 333 30 Y.G. Zheng, H.F. Ye, Z.Q. Zhang and H.W. Zhang, *Phys. Chem. Chem. Phys.*, 2012, 14,
334 964-971.